

Design, Synthesis, Spectral Characterization, DNA Binding and Antibacterial Studies of Ternary Metal Complexes with 1,10-Phenanthroline and 2-Acetylthiophene-4-phenyl-3-thiosemicarbazone

Kummara Srinivasulu¹, Katreddi Hussain Reddy^{1,*}, Kandukuri Anuja¹, Dornala Dhanalakshmi¹ and Yamaduru Balaramaiah Nagamani²

¹Department of Chemistry, Sri Krishnadevraya University, Ananthapuramu 515003, India

²Department of Chemistry, Government Degree College for Women, Hindupur 515201, India

(* Corresponding author's e-mail: khussainreddy@yahoo.co.in)

Received: 8 June 2021, Revised: 25 October 2021, Accepted: 8 November 2021

Abstract

Bivalent metal complexes having the composition $M(\text{Phen})\text{Cl}_2$ (where, $M = \text{Cu}(\text{II}), \text{Ni}(\text{II})$ and $\text{Co}(\text{II})$; $\text{Phen} = 1,10\text{-Phenanthroline}$) are reacted with 2-acetylthiophene-4-phenyl-3-thiosemicarbazone (ATPT) to produce ternary complexes with molecular formula $[M(\text{Phen})(\text{ATPT})\text{Cl}_2] \cdot \text{H}_2\text{O}$. The complexes are characterized using physical (molar conductivity) and spectral (mass spectra, infrared and electronic spectroscopies) methods. Electrochemical behavior of complexes was uncovered using cyclic voltammetry. DNA binding properties of the complexes are determined by using absorption UV-Visible spectrophotometry. Metal complexes are screened for their antibacterial activity by using agar well diffusion method against pathogenic bacterial strains viz. Gram-ve such as *Escherichia coli*, *Klebsiella Pneumonia* and Gram+ve such as *Staphylococcus aureus*, *Bacillus cereus*. The $[\text{Ni}(\text{Phen})(\text{ATPT})\text{Cl}_2] \cdot 0.5 \text{H}_2\text{O}$ complex inhibits bacteria more stronger than any other complex.

Keywords: 2-Acetylthiophene-4-phenyl-3-thiosemicarbazone, Ternary transition metal complexes, Cyclic voltammetry, DNA binding, Antibacterial activity

Introduction

Sulphur has been used in a medicinal context since antiquity. It is one of the earliest known elements and was known to the Greeks to have healing power. Magnesium sulphate was the 1st sulphur-containing compound approved by the Food and Drug Administration (FDA), and sulphur-containing compounds were the hallmarks of several antibiotic breakthroughs that brought man into the modern antibiotic era. Several Nobel Prizes have been awarded for work done on sulphur-containing drugs. Sulphur containing compounds continue to represent a large portion of new FDA approvals.

Thiosemicarbazones are important class of sulphur containing ligands for the synthesis and characterization of transition metal complexes [1,2]. These ligands are extensively used as chromogenic reagents for the spectrophotometric determination of transition metal ions [3]. Transition metal complexes with heterocyclic thiosemicarbazones are expected to exhibit interesting stereochemical, electrochemical, and electronic properties [4,5]. Metal complexes of Phenanthroline (Phen) are known to function as potential anti-tumor agents [6].

Recently, mixed ligand metal complexes with Schiff bases as a main ligand Phen as a co-ligand are reviewed [7]. But no report is available in the literature [8-10] on mixed ligand metal complexes with Phen and 2-Acetylthiophene-4-phenyl-3-thiosemicarbazone(ATPT). The ligand was synthesized, characterized [11,12] and was used in our laboratory for the spectrophotometric determination of copper(II) in alloys, edible oils and seeds [13]. However, transition metal complexes with Phen as primary ligand and thiosemicarbazone as secondary ligand are not investigated so far [14].

Mixed ligand complexes of biologically important compounds may serve as models for biochemical processes [15,16]. We have studied [17-19] deoxyribonucleic acid binding and antibacterial activity of various transition metal complexes recently to develop antimicrobial agents. To renew our interests, herein we communicate our results on spectral characterization, DNA Binding and Antibacterial activity studies of ternary metal complexes with Phen and ATPT. The main objective of this work is to bring correlation between DNA binding and bacteria inhibition of complexes.

Materials and methods

4-phenyl-3-thiosemicarbazide, 2-Acetylthiophene and Phen, were purchased from Sigma-Aldrich. Elemental analyses were carried out on a Heraeus Vario EL III Carlo Erba 1108 instrument. Molar conductivity measurements at $298 \pm 2\text{K}$ in dry and purified DMF were carried out using a CM model 162 conductivity cell (ELICO). ESR spectra were recorded on a Varian E-112 X-band spectrophotometer at room temperature (RT) and liquid nitrogen temperature (LNT) in solution (DMF) state. Cyclic voltammetric measurements were taken on degassed (N_2 bubbling for 5 min) solutions (10^{-3} M) containing $0.1\text{ M Bu}_4\text{NPF}_6$ as the supporting electrolyte.

Preparation of ATPT

The ligand, ATPT was prepared using 4-phenyl-3-thiosemicarbazide and 2-Acetylthiophene. Ethanolic solutions of 4-phenyl-3-thiosemicarbazide (5 mmol), and 2-Acetylthiophene (5 mmol) were combined in a round bottom flask. Two drops of CH_3COOH were added and the reaction mixture was refluxed for 3 h and cooled to room temperature. The compound was obtained as shiny milk white crystalline product, which was subsequently used in the synthesis of metal complexes. Yield 83 %, M. Pt. $180 - 182\text{ }^\circ\text{C}$, IR spectra (cm^{-1}) 3297, 1589, 1194 cm^{-1} are assigned to $\nu(\text{N-H asym})$, $\nu(>\text{C}=\text{N})$ and $\nu(>\text{C}=\text{S})$ stretching vibrations respectively. NMR spectra (δ , in ppm) 9.31 (singlet 1H), 8.70 (singlet 1H), 7.25 - 7.44 (multiplet 5H), 7.71 (doublet 3H), 7.06 (doublet of doublet 3H), 2.34 (singlet 3H) are assigned to $>\text{NH}$, phenyl, thiophene H and CH_3 protons respectively. In the mass spectrum of ATPT, the molecular ion peak value coincides with its formula weight, 275. Mass spectrum of ATPT ligand is shown in **Figure 1**.

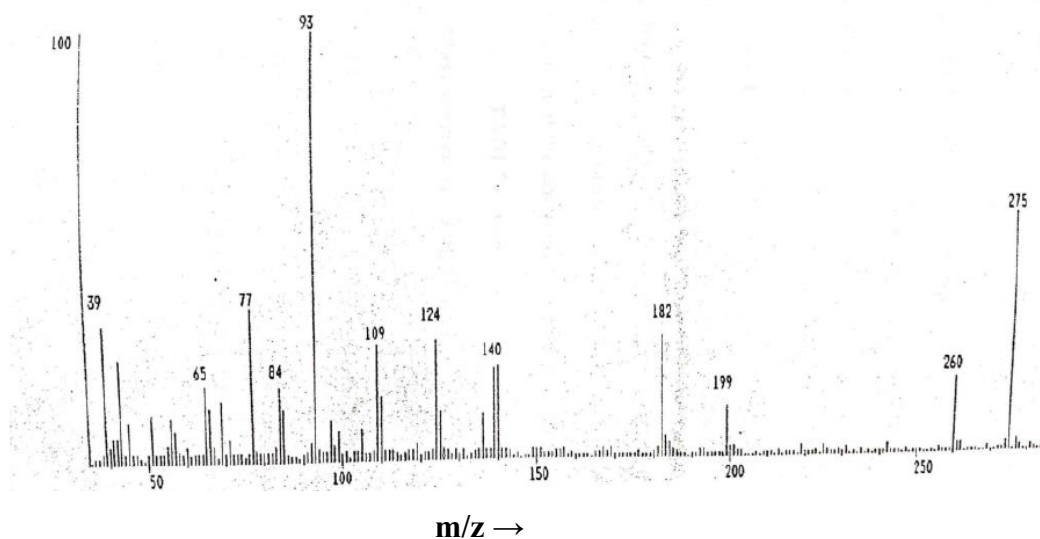


Figure 1 Mass spectrum of ATPT ligand.

Based on the positions of peaks (**m/z values**) in the mass spectrum, fragmentation of pattern of ATPT is shown in **Figure 2**.

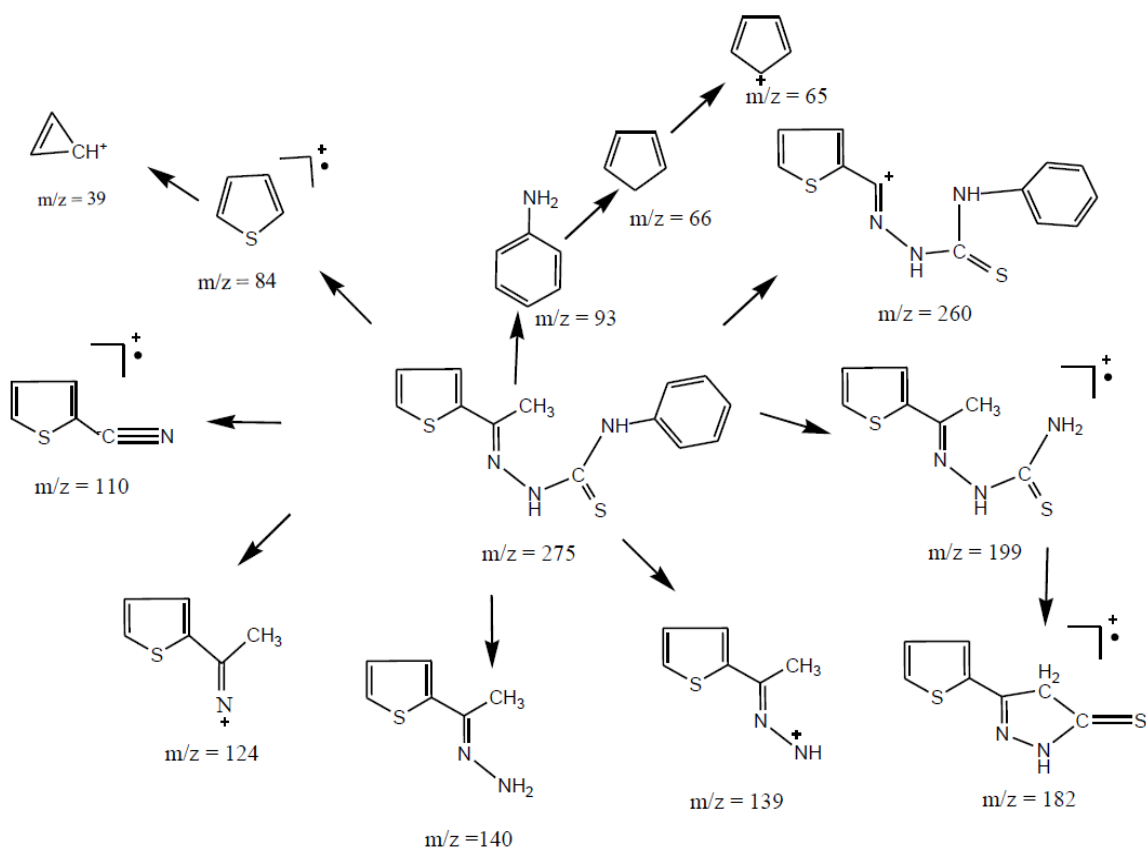


Figure 2 Mass spectral fragmentation of ATPT ligand.

Preparation of mixed ligand metal complexes

A 1.2 g of ATPT ligand (0.006 moles) was dissolved in 15 mL of 0.05 N NaOH in methanol solvent in 100 mL beaker. A 1.0 g Cu (Phen)₂Cl₂ (0.003 moles) was dissolved in 15 mL of methanol solvent in 100 mL beaker. Ligand solution and Cu(Phen)₂Cl₂ solution were transferred into 100 mL round bottom flask and heated under reflux for 1 h. On cooling the contents of flask, light green coloured complex was formed. It was collected by filtration, washed with small quantities of methanol and dried in air. Ni(Bpy)(ATPT)Cl₂ and Co(Bpy)(ATPT)Cl₂ complexes were prepared similarly.

Results and discussion

Physico-chemical and analytical studies

Metal complexes having the composition M(Phen)₂Cl₂ (Where, M = Co(II), Ni(II) and Cu(II); Phen = 1,10-Phenanthroline) are reacted with ATPT to produce heteroleptic transition metal complexes with molecular formula [M(Phen)(ATPT)Cl₂]·H₂O. All the complexes are stable at room temperature, non-hygroscopic, insoluble in water, slightly soluble in methanol and ethanol but readily soluble in DMF and DMSO. Molecular weights of the complexes are determined based on their ESI-mass spectra. ESI-mass spectrum of [Co(Phen)(ATPT)Cl₂]·0.5 H₂O complex is shown in **Figure 3**. The physico-chemical data for the complexes are summarized in **Table 1**.

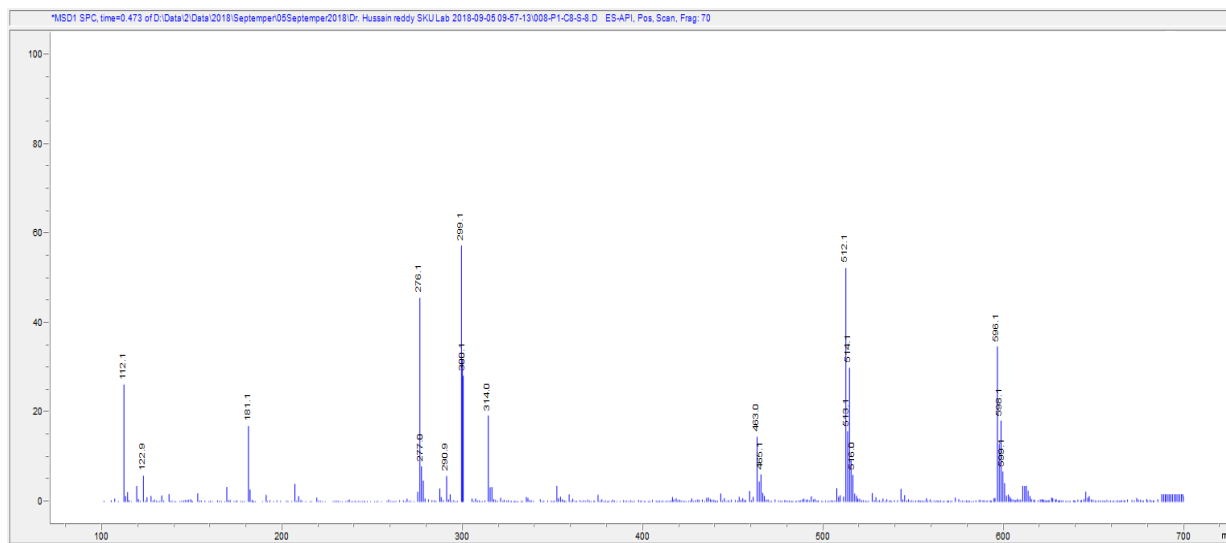


Figure 3 ESI-Mass spectrum of $[\text{Co}(\text{Phen})(\text{ATPT})\text{Cl}_2] \cdot 0.5 \text{H}_2\text{O}$ complex.

Conductivity measurements

Analytical data support the compositions of the complexes. For 1:1 electrolyte the molar conductivity values are in the range $65 - 90 \Omega^{-1} \text{cm}^2 \text{mol}^{-1}$ in dimethylformamide (DMF). The observed values ($18 - 25 \Omega^{-1} \text{cm}^2 \text{mol}^{-1}$) indicate non-electrolytic nature of complexes [20].

Table 1 Physicochemical and analytical data of Cu(II), Ni(II) and Co(II) complexes.

S. No	Complex	ESI-MS (F.W)	Melting point (°C)	Colour (Yield %)	Elemental composition Found (Calcd.) (%)			Molar Conductivity ($\Omega^{-1} \text{cm}^2 \text{mol}^{-1}$)
					C	H	N	
1	$[\text{Cu}(\text{Phen})_2\text{Cl}_2]$	498 (496)	Above 300	Light Green (72.98 %)	58.15 (58.06)	3.20 (3.22)	11.15 (11.29)	18
2	$[\text{Cu}(\text{Phen})(\text{ATPT})\text{Cl}_2] \cdot \text{H}_2\text{O}$	608 (608)	264 - 265	Brown (81.58 %)	49.15 (49.34)	3.82 (3.78)	11.55 (11.51)	19
3	$[\text{Ni}(\text{Phen})_2\text{Cl}_2]$	491 (491)	Above 300	Light Blue (73.72 %)	58.73 (58.65)	3.24 (3.25)	11.34 (11.40)	20
4	$[\text{Ni}(\text{Phen})(\text{ATPT})\text{Cl}_2] \cdot 0.5 \text{H}_2\text{O}$	596 (595)	292 - 293	Light Green (82.55 %)	50.50 (50.42)	3.90 (3.86)	11.75 (11.76)	25
5	$[\text{Co}(\text{Phen})_2\text{Cl}_2]$	492 (492)	Above 300	Light Blue (74.50 %)	58.65 (58.53)	3.30 (3.25)	11.43 (11.38)	18
6	$[\text{Co}(\text{Phen})(\text{ATPT})\text{Cl}_2] \cdot 0.5 \text{H}_2\text{O}$	598 (596)	288 - 289	Brown (82.27 %)	50.25 (50.33)	3.82 (3.85)	11.65 (11.74)	21

Electronic spectra

The electronic spectra of the complexes are recorded in DMF and data are presented in **Table 2**. A strong and sharp peak is observed in the region of $37,313 - 31,250 \text{cm}^{-1}$ due to $\pi \rightarrow \pi^*$ transition of aromatic chromophore [21]. Medium intensity bands observed in the range of $30,303 - 27,472 \text{cm}^{-1}$ are assigned to which correspond to $\text{M} \rightarrow \text{L}$ charge transfer transition [22]. A weak band in the region of $16,611 - 13,245 \text{cm}^{-1}$ region may be assigned to d-d transitions.

Table 2 Electronic spectral data for Cu(II), Ni(II) and Co(II) complexes.

S. No	Complex	λ max (nm)	Frequency (cm^{-1})	Assignment
1	Cu(Phen) ₂ Cl ₂	295	33,898	$\pi \rightarrow \pi^*$ transition
		330	30,303	M \rightarrow L CT
		755	13,245	d-d transition
2	[Cu(Phen)(ATPT)Cl ₂] H ₂ O	320	31,250	$\pi \rightarrow \pi^*$ transition
		364	27,472	M \rightarrow L CT
		602	16,611	d-d transition
		327	30,581	M \rightarrow L CT
3	Ni(Phen) ₂ Cl ₂	345	28,985	d-d transition
		627	15,948	d-d transition
		990	10,101	d-d transition
4	[Ni(Phen)(ATPT)Cl ₂] 0.5 H ₂ O	336	29,761	M \rightarrow L CT
		290	34,482	$\pi \rightarrow \pi^*$ transition
5	Co(Phen) ₂ Cl ₂	351	28,490	d-d transition
		608	16,447	d-d transition
		677	14,771	d-d transition
6	[Co(Phen)(ATPT)Cl ₂] 0.5 H ₂ O	268	37,313	$\pi \rightarrow \pi^*$ transition
		365	27,397	M \rightarrow L CT

Infrared spectra

Infrared (IR) spectral data of ATPT and its metal complexes and assignment of peaks are given in **Table 3**. A strong band is observed in the IR spectrum of ATPT at 1593 cm^{-1} which is assigned to $\nu(> \text{C}=\text{N})$ group. In all the complexes, this band is shifted to lower frequency indicating the participation of azomethine nitrogen atom in coordination [23,24]. A medium band is appeared in the spectrum of ATPT at 1194 cm^{-1} , which is assigned to $\nu(\text{C}=\text{S})$ group. This band is shifted to lower wave number suggesting participation thioketo sulphur in chelation. Thiophene ring deformation modes are observed around 710 and 610 cm^{-1} . These bands are shifted to higher wave number indicating coordination of thiophene sulphur to metal. In far IR region, new peaks are observed in $550 - 585$ and $457 - 467 \text{ cm}^{-1}$ regions which are assigned to $\nu\text{M-N}$ and $\nu\text{M-S}$ vibrations [25,26] respectively.

Table 3 IR spectral bands (cm^{-1}) of Cu(II), Ni(II) and Co(II) complexes.

ATPT	[Cu(Phen)(ATPT)]Cl ₂ H ₂ O	[Ni(Phen)(ATPT)]Cl ₂ 0.5 H ₂ O	[Co(Phen)(ATPT)] Cl ₂ 0.5 H ₂ O	Assignment
1589	1548	1557	1562	$\nu\text{C}=\text{N}$)
	1485	1479	1475	$\nu\text{C-C}$
	1305	1315	1338	(thiophene)
1194	1158	1145	1142	$\nu\text{C}=\text{S}$
				(thione)
	1025	1032	1027	
	858	857	849	
710	720	730	728	
610	630	628	621	
	585	550	575	$\nu\text{M-N}$
	465	467	457	$\nu\text{M-S}$

ESR spectra

ESR spectra of copper complexes were recorded in DMF solution at room temperature and at liquid nitrogen temperature. ESR spectra of $[\text{Cu}(\text{Phen})(\text{ATPT})\text{Cl}_2] \cdot \text{H}_2\text{O}$ recorded at LNT are shown in **Figure 4**. The spin Hamiltonian, orbital reduction and bonding parameters of complexes are given in **Table 4**.

Table 4 ESR spectral data of complexes.

Parameter	$\text{Cu}(\text{Phen})_2\text{Cl}_2$		$[\text{Cu}(\text{Phen})(\text{ATPT})\text{Cl}_2\text{H}_2\text{O}$	
	LNT	RT	LNT	RT
g_{\parallel}	2.26	2.23	2.16	2.12
g_{\perp}	2.05	2.16	2.06	2.09
g_{ave}	2.12	2.21	2.15	2.01
G	0.51	0.69	0.71	0.95
$A_{\parallel} \times 10^{-5}$	0.00104	-	0.00123	-
$A_{\perp} \times 10^{-5}$	-	-	0.00932	-
K_{\parallel}	0.991	-	0.087	-
K_{\perp}	1.061	-	0.059	-
λ	432	-	419	-
α	0.366	-	0.245	-

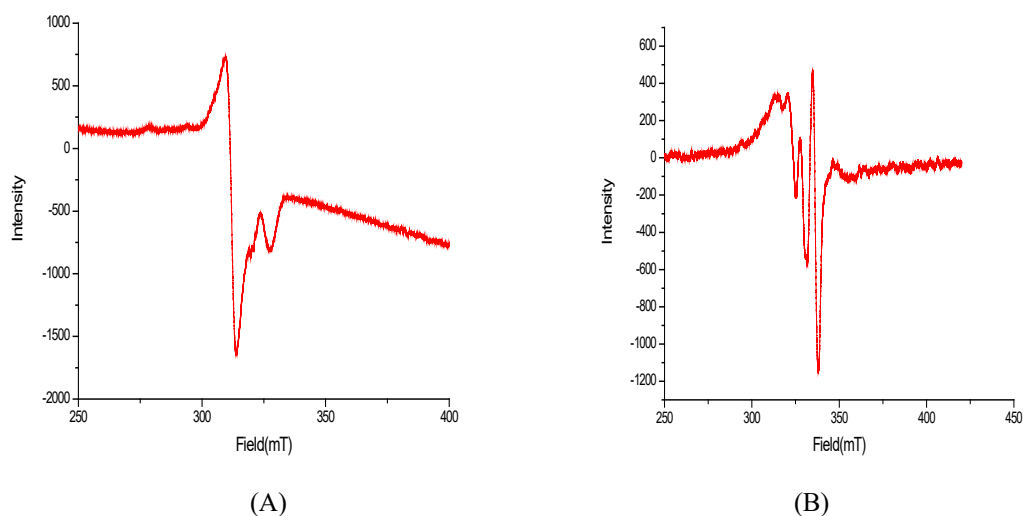


Figure 4 ESR spectra of $[\text{Cu}(\text{Phen})(\text{ATPT})\text{Cl}_2] \cdot \text{H}_2\text{O}$ complex (A) at LNT and (B) at RT.

The g_{\parallel} and g_{\perp} are computed from the spectra using tetracyanoethylene (TCNE) free radical as **g** marker. The observed g_{\parallel} values for complexes are less than or equal to 2.3 suggesting significant covalent character of metal ligand bond in agreement with observation of Kivelson and Neiman [27]. The g_{\parallel} and g_{\perp} were more than 2, corresponding to an axial symmetry. The trend $g_{\parallel} > g_{\perp} > g_e$ (2.0023) observed for these complexes suggests that the unpaired electron is localized in the $d_{x^2-y^2}$ orbital of the copper ion. The axial symmetry parameter G is defined as:

$$G = \frac{[g_{\parallel} - 2.0023]}{[g_{\perp} - 2.0023]} \quad (1)$$

The calculated G values for these complexes are less than 4.0 which indicates the presence of small exchange coupling and misalignment of molecular axes. The g_{\parallel} , g_{\perp} , A_{\parallel} , A_{\perp} of complexes and the energies of the d-d transitions are used to calculate the orbital reduction parameters (K_{\parallel} , K_{\perp}), the bonding parameter (α^2). The factor α^2 which is usually taken as a measure of covalence and it is evaluated by the expression:

$$\alpha^2 = -A_{\parallel}/p + (g_{\parallel} - 2.0023) + 3/7(g_{\perp} - 2.0023) + 0.04 \quad (2)$$

Hathaway pointed out that for pure σ bonding $K_{\parallel} \approx K_{\perp} \approx 0.77$, for in-plane π -bonding $K_{\parallel} < K_{\perp}$, while out of plane π -bonding $K_{\parallel} > K_{\perp}$ the following simplified expressions were used to calculate K_{\parallel} and K_{\perp} :

$$K_{\parallel}^2 = (g_{\parallel} - 2.0023)/8 \times \lambda_0 \text{ X d-d transition} \\ K_{\perp} = (g_{\perp} - 2.0023)/8 \times \lambda_0 \text{ X d-d transition} \quad (3)$$

The observed $K_{\parallel} < K_{\perp}$ relation for $\text{Cu}(\text{phen})_2\text{Cl}_2$ complex indicates the significant in plane π -bonding and $K_{\parallel} > K_{\perp}$ relation for $[\text{Cu}(\text{Phen})(\text{ATPT})\text{Cl}_2] \cdot 0.5 \text{H}_2\text{O}$ complex indicates the out of plane π -bonding.

Cyclic voltammetry

Electrochemical properties of complexes are investigated by using cyclic voltammetry, Voltammograms of complexes are recorded in DMF using 0.1 M tetrabutylammonium hexafluorophosphate as supporting electrolyte. The cyclic voltammogram of $[\text{Co}(\text{Phen})(\text{ATPT})\text{Cl}_2] \cdot 0.5 \text{H}_2\text{O}$ complex is shown in **Figure 5** and the electrochemical data of complexes are summarized in **Table 5**.

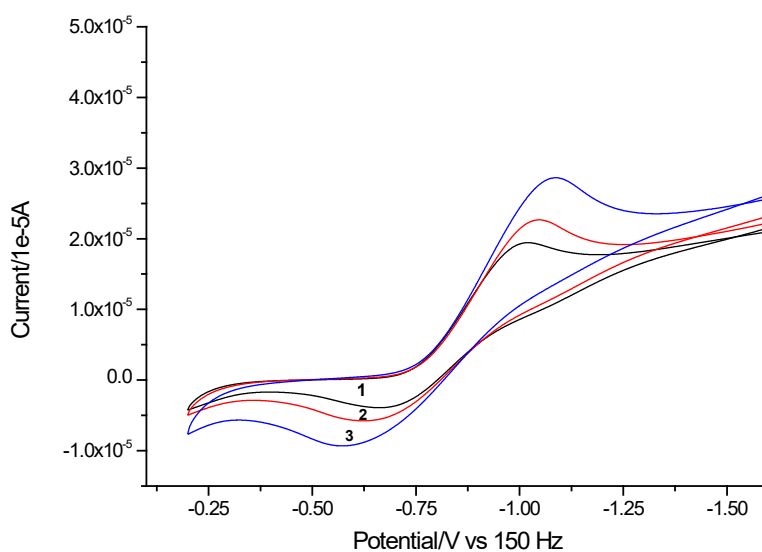


Figure 5 Cyclic voltammogram of $[\text{Co}(\text{Phen})(\text{ATPT})\text{Cl}_2] \cdot 0.5 \text{H}_2\text{O}$ at different scan rates (1) 0.05 (2) 0.1 and (3) 0.2 mVs^{-1} .

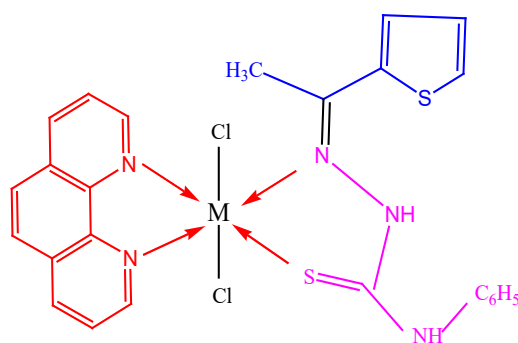
Table 5 CV data of Cu(II), Ni(II) and Co(II) complexes.

S. No	Complex	E _{pc}	E _{pa}	ΔE _p (mv)	E _{1/2}	-i _c /i _a	Log K _c ^a	-ΔG ^b
1	Cu(Phen) ₂ Cl ₂	-0.086	0.140	226	0.113	1.461	0.0148	854
2	[Cu(Phen)(ATPT)]Cl ₂ H ₂ O	-0.096	0.125	221	0.110	1.770	0.0151	877
3	Ni(Phen) ₂ Cl ₂	-1.83	-0.680	115	-1.25	1.317	0.0292	168
4	[Ni(Phen)(ATPT)] Cl ₂ 0.5 H ₂ O	-1.070	-0.686	384	-0.878	1.981	0.0874	218
5	Co(Phen) ₂ Cl ₂	-1.21	-0.55	660	-0.880	1.261	0.0508	293
6	[Co(Phen)(ATPT)] Cl ₂ 0.5 H ₂ O	-1.017	-0.670	347	-0.843	1.612	0.0967	558

^alog K_c = 0.434ZF/RTΔE_p; ^bΔG° = -2.303RT log K_c.

Stability constants of complexes are calculated using ΔE_p values. Stability of complexes may be predicted based on standard free energy change (ΔG) values. The ΔG values are higher for mixed ligand complexes. Data suggest that mixed ligand complexes are more stable than the parent [M(Phen)Cl₂] complexes.

Repeated scans at various scan rates suggest that the presence of stable redox species in solution. It has been observed that cathodic (I_{pc}) and anodic (I_{pa}) peak currents were not equal. The calculated E_{1/2} values for Cu(Phen)₂Cl₂ and Cu(Phen)(ATPT)]Cl₂H₂O are 0.113 and 0.110 V respectively. It may be concluded that all the bivalent metal complexes undergo 1 electron reduction to their respective M(I) complexes. The non-equivalent currents in cathodic and anodic peaks indicate quasi-reversible behaviour [28]. The difference, ΔE_p for all the complexes is better than the Nerstian requirement 59/n mV (n = number of electrons involved in oxidation reduction). The ΔE_p values indicate quasi-reversible character of electron transfer [29]. The complexes show large separation between anodic and cathodic peaks indicating quasi-reversible character. Based on analytical, physicochemical and spectral data, a general structure (**Figure 6**) is proposed for the complexes.

**Figure 6** Proposed structure of ternary complexes. [M = Cu(II), Ni(II) and Co(II)].

DNA binding studies

The binding interaction of the complexes with DNA was monitored by comparing their absorption spectra with and without CT-DNA. Absorption spectra of [Co(Phen)(ATPT)] Cl₂ 0.5 H₂O complex in the absence and in the presence of CT-DNA are shown in **Figure 7**. It has been observed (**Table 6**) that molar absorptivity of complexes decreases (hypochromism, Δε, +20.79 % to +38.07; and absorption maximum is shifted towards higher wavelength (bathochromic shift Δλ = 0.5 - 1.5) upon each addition of CT-DNA.

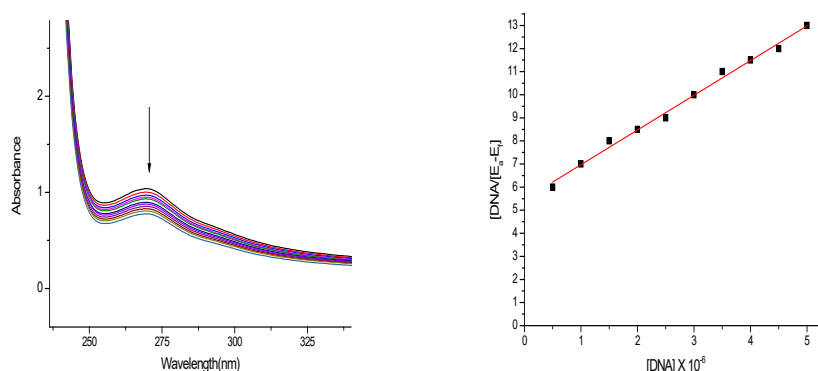


Figure 7 (A) Absorption Spectra of $[\text{Co}(\text{Phen})(\text{ATPT})\text{Cl}_2] 0.5 \text{H}_2\text{O}$ in the absence and in the presence of increasing concentration of CT-DNA; [The top most spectrum is recorded in the absence of CT-DNA and below spectra on addition 20 μL DNA each time]. (B) A plot $[\text{DNA}]/(E_a-E_f)$ vs $[\text{DNA}] \times 10^{-6}$ is shown.

Table 6 Electronic absorption data upon addition of CT-DNA to the complex.

S. No	Complexes	$\lambda \text{ max}(\text{nm})$		$\Delta \lambda$	H %	Kb [M^{-1}]
		Free	Bound			
1	$\text{Cu}(\text{Phen})_2\text{Cl}_2$	269.0	270.0	1.0	20.79	1.44×10^5
2	$[\text{Cu}(\text{Phen})(\text{ATPT})]\text{Cl}_2\text{H}_2\text{O}$	271.0	272.0	1.0	38.07	5.25×10^5
3	$\text{Ni}(\text{Phen})_2\text{Cl}_2$	270.0	270.5	0.5	15.83	1.26×10^5
4	$[\text{Ni}(\text{Phen})(\text{ATPT})]\text{Cl}_2 0.5 \text{H}_2\text{O}$	268.0	269.5	1.5	35.89	1.42×10^5
5	$\text{Co}(\text{Phen})_2\text{Cl}_2$	269.5	270.5	1.0	12.19	1.73×10^5
6	$[\text{Co}(\text{Phen})(\text{ATPT})]\text{Cl}_2 0.5 \text{H}_2\text{O}$	272.0	273.0	1.0	21.74	4.14×10^5

The intrinsic binding constants of complexes are given in **Table 6**. Hyperchromic effect and hypochromic effect are the special features of DNA concerning its double helix structure. Hypochromism results from the contraction of DNA in the helix axis as well as from the change in conformation on DNA while hyperchromism emerges from the damage of the double helix structure. Hypochromism and bathochromic shift suggest that these complexes bind DNA through intercalation involving a strong π -stacking interaction between the aromatic chromophore and base pairs of DNA [30].

Antibacterial activity

The diameters of inhibition of zones were measured with Verniercallipers in mm and its values are depicted in the **Table 7**. Antibacterial activity of present complexes is compared (**Figure 8**) with the reference compound, ciprofloxacin. The reference compound shows higher activity even in the presence of its smaller quantities (5 $\mu\text{g}/\mu\text{L}$). However, all the complexes show significant antibacterial activity with its higher amounts (100 - 300 $\mu\text{g}/\mu\text{L}$).

The zone of inhibition data suggest that the $[\text{Ni}(\text{Phen})(\text{ATPT})]\text{Cl}_2 0.5 \text{H}_2\text{O}$ complex inhibits bacteria more strongly than any other complex. Further, the mixed ligand complex, for example $[\text{Ni}(\text{Phen})(\text{ATPT})]\text{Cl}_2 0.5 \text{H}_2\text{O}$ complex shows more activity than the parent complex $\text{Ni}(\text{Phen})_2\text{Cl}_2$ possibly due to the synergistic effect of Phen and ATPT ligands against bacteria.

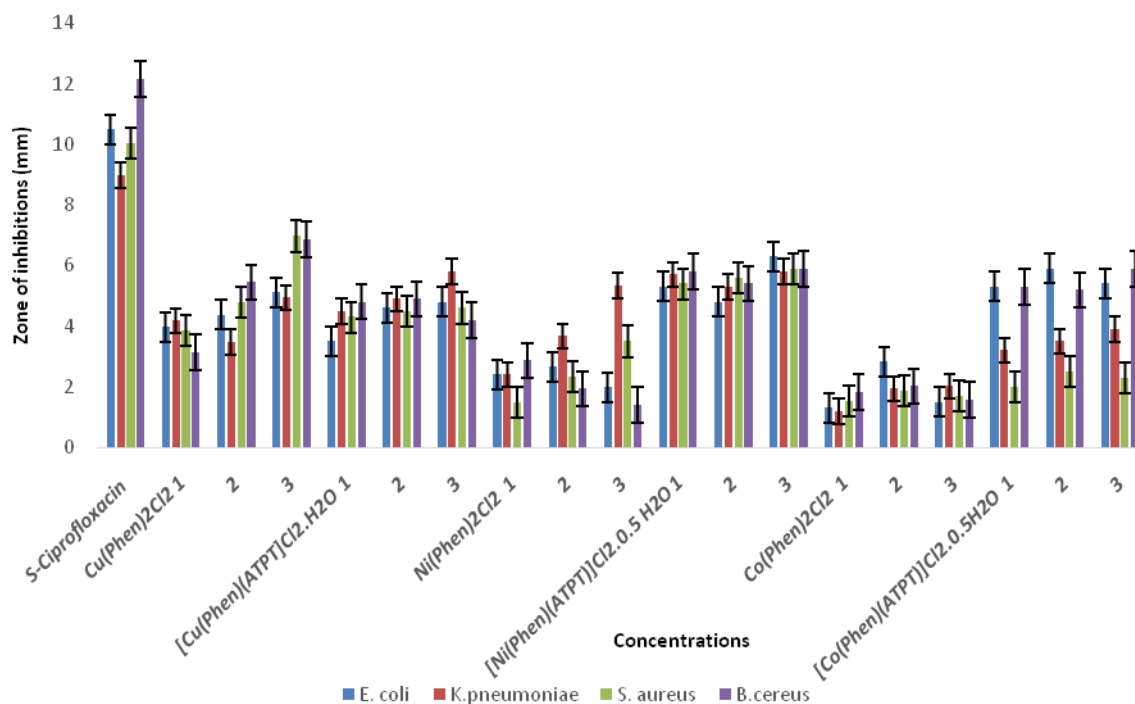


Figure 8 Graphical representation of antibacterial activity of metal complexes against pathogenic bacterial strains. (1 - 100; 2 - 200; 3 - 300 $\mu\text{g}/\mu\text{L}$).

Table 7 Antibacterial activity of different metal complexes against pathogenic bacterial strains.

S. No	Sample	Treatment (Concentration) ($\mu\text{g}/\mu\text{L}$)	E. coli (Mean \pm SE)	K. pneumoniae (Mean \pm SE)	S. aureus (Mean \pm SE)	B. cereus (Mean \pm SE)
1	S-Ciprofloxacin	5	10.5 \pm 0.02	8.98 \pm 0.09	10.03 \pm 0.03	12.16 \pm 0.05
2	Cu(Phen) ₂ Cl ₂	100	3.98 \pm 0.14	4.17 \pm 0.17	3.87 \pm 0.18	3.14 \pm 0.25
		200	4.37 \pm 0.47	3.47 \pm 0.47	4.8 \pm 0.32	5.45 \pm 0.75
		300	5.12 \pm 0.8	4.93 \pm 0.3	6.97 \pm 0.06	6.87 \pm 0.36
3	[Cu(Phen)(ATPT)]Cl ₂ .H ₂ O	100	3.5 \pm 0.03	4.5 \pm 0.07	4.3 \pm 0.07	4.8 \pm 0.07
		200	4.6 \pm 0.04	4.9 \pm 0.08	4.5 \pm 0.09	4.9 \pm 0.05
		300	4.8 \pm 0.08	5.8 \pm 0.09	4.6 \pm 0.25	4.2 \pm 0.36
4	Ni(Phen) ₂ Cl ₂	100	2.4 \pm 0.11	2.4 \pm 0.17	1.5 \pm 0.28	2.87 \pm 0.16
		200	2.67 \pm 0.09	3.67 \pm 0.17	2.34 \pm 0.15	1.93 \pm 0.26
		300	1.98 \pm 0.06	5.33 \pm 0.17	3.5 \pm 0.63	1.4 \pm 0.32
5	[Ni(Phen)(ATPT)] Cl ₂ .0.5 H ₂ O	100	5.3 \pm 0.07	5.7 \pm 0.07	5.4 \pm 0.36	5.8 \pm 0.67
		200	4.8 \pm 0.08	5.3 \pm 0.06	5.6 \pm 0.01	5.4 \pm 0.89
		300	6.3 \pm 0.01	5.8 \pm 0.07	5.9 \pm 0.06	5.9 \pm 0.35
6	Co(Phen) ₂ Cl ₂	100	1.3 \pm 0.15	1.2 \pm 0.18	1.53 \pm 0.3	1.83 \pm 0.01
		200	2.83 \pm 0.17	1.93 \pm 0.13	1.87 \pm 0.87	2.01 \pm 0.34
		300	1.5 \pm 0.29	2.01 \pm 0.15	1.69 \pm 0.23	1.57 \pm 0.36
7	[Co(Phen)(ATPT)] Cl ₂ .0.5 H ₂ O	100	5.3 \pm 0.04	3.2 \pm 0.24	2 \pm 0.32	5.3 \pm 0.01
		200	5.9 \pm 0.09	3.5 \pm 0.05	2.5 \pm 0.89	5.2 \pm 0.05
		300	5.4 \pm 0.06	3.9 \pm 0.07	2.3 \pm 0.47	5.9 \pm 0.14

Conclusions

Mixed ligand transition metal complexes with Phen and ATPT are synthesized and characterized based on ESI mass spectra, molar conductivity, infrared and electronic spectroscopy. Electrochemical properties of complexes are uncovered by using cyclic voltammetry. The complexes show quasi-reversible cyclic voltammetric responses for the M(II)/M(I) couple. The binding properties of these complexes with calf-thymus DNA are investigated by using absorption spectrophotometry. Mixed ligand metal complexes show high binding affinity towards DNA. Metal complexes are screened for their antibacterial activity by using agar well diffusion method against pathogenic bacterial strains. Although antibacterial activity of present complexes is less than the reference compound (Ciprofloxacin), the mixed ligand compounds show significant activity when taken in higher amounts (100 - 300 µg/µL).

Acknowledgements

KHR is thankful to UGC for the award of UGC-BSR Faculty Fellowship. The authors also thank UGC and DST for providing equipment facility under SAP and FIST programs respectively. The authors also thank Karunya Institute of Technology and Sciences, Coimbatore for sending ESI-Mass spectral data of complexes.

References

- [1] MJM Campbell. Transition metal complexes of thiosemicarbazide and thiosemicarbazones. *Coord. Chem. Rev.* 1975; **15**, 279-319.
- [2] S Padhye and GB Kauffman. Transition metal complexes of semicarbazones and thiosemicarbazones. *Coord. Chem. Rev.* 1985; **63**, 127-60.
- [3] KH Reddy and DV Reddy. Analytical data comparison of analytical potentialities of thiosemicarbazones and semicarbazones. *Quarterly Chem. Rev.* 1985; **1**, 47-98.
- [4] PM Krishna and KH Reddy. Synthesis, single crystal structure and DNA cleavage studies on first ⁴N-ethyl substituted three coordinate copper(I) complex with thiosemicarbazone. *Inorg. Chim. Acta* 2009; **362**, 4185-90.
- [5] PR Haribabu and KH Reddy. DNA binding and cleavage activity of cationic dinuclear copper(II) and nickel(II) complexes with novel oxime-thiosemicarbazones. *Indian J. Chem.* 2011; **50A**, 996-1001.
- [6] Y Prashanthi, K Kiranmai and K Sathishkumar. Spectroscopic characterization and biological activity of mixed ligand complexes of Ni(II) with 1,10-phenanthroline and heterocyclic Schiff bases. *Bioinorg. Chem. Appl.* 2012; **2012**, 948534.
- [7] R Mahalakshmi and N Raman. A therapeutic journey of mixed ligand complexes containing 1,10-phenanthroline derivatives: A review. *Int. J. Curr. Pharm. Res.* 2016; **8**, 1-6.
- [8] KH Sugiyarto, C Kusumawardani, H Wigati and H Sutrisno. structural study of the powder complex of Cu(II)-1,10-phenanthroline- trifluoroacetate. *Orient. J. Chem.* 2019; **35**, 325-31.
- [9] A Oveisikeikha and H Saravani. Synthesis and characterization of new binuclear chromium, cadmium complexes based on terpyridine and phenanthroline. *Orient. J. Chem.* 2018; **34**, 1323-7.
- [10] RKR Al-shemary, LKA Karem and FH Ghanim. Structure, and in vitro antimicrobial and antifungal evaluation of some amino benzoic acids, derived ligand Schiff base and their mixed complexes with Cu(II), Hg(II), Mn(II), Ni(II) and Co(II). *Orient. J. Chem.* 2018; **34**, 1105-13.
- [11] NBL Prasad. 2001, Spectrophotometric determination of Cu(II) and Ni(II) in edible oils using oxime-thiosemi-carbazones. Master Thesis. Sri Krishnadevaraya University, India.
- [12] GMD Lima, JL Neto, H Beraldo, HGL Siebald and DJ Duncalf. Structural and spectral studies of thiosemicarbazones derived from 2-acetylthiophene. *J. Mol. Struct.* 2002; **604**, 287-91.
- [13] M SayajiRao, NBL Prasad and KH Reddy. Spectrophotometric determination of copper(II) in alloys and edible oils using 2-acetylthiophene thiosemicarbazone. *Indian J. Chem.* 2006; **45A**, 1659-62.
- [14] VS Shivankar, RB Vaidya, SR Dharwadkar and NV Thakkar. Synthesis, characterization and biological activity of mixed ligand Co(II) complexes of 8-hydroxyquinoline and some amino acids. *Synth. React. Inorg. Met. Org. Chem.* 2003; **33**, 1597-622.
- [15] A Adkhis, S Djebbar, O Benali-Baitich, A Kadir, MA Khan and G Bouet. Synthesis, characterization, and electrochemical behavior of mixed-ligand complexes of cobalt(III) with dimethylglyoxime and some amino acids. *Synth. React. Inorg. Met. Org. Chem.* 2003; **33**, 35-50.
- [16] KH Reddy. *Bioinorganic chemistry*. New Age International Publishers, New Delhi, India, 2020.

- [17] D Dornala, HR Katreddi, A Kandukuri, S Kummara and NY Balaramaiah. Synthesis, characterization, deoxyribonucleic acid binding and antimicrobial activity of bivalent metal complexes with 2-acetylpyridine isonicotinoylhydrazone. *J. Appl. Pharm. Sci.* 2021; **11**, 84-92,
- [18] YB Nagamani, KH Reddy, K Srinivasulu, D Dhanalakshmi and K Anuja. Antibacterial activity and DNA binding properties of bivalent metal complexes with cuminaldehyde benzoylhydrazone (CABH). *Int. J. Pharm. Res.* 2021; **12**, 188-95.
- [19] D Dhanalakshmi, KH Reddy, K Srinivasulu, K Anuja, YB Nagamani and P Shravya. DNA binding and antibacterial activity studies on transition metal complexes with 2-formylpyridine isonicotinoyl hydrazone. *Res. J. Chem. Environ.* 2020; **24**, 130-40.
- [20] WJ Geary. The use of conductivity measurements in organic solvents for the characterization of coordination compounds. *Coord. Chem. Rev.* 1971; **7**, 81-122.
- [21] C Tu, X Wu, Q Liu, X Wang, Q Xu and Z Guo. Crystal structure, DNA-binding ability and cytotoxic activity of platinum (II) 2,2'-dipyridylamine complexes. *Inorg. Chim. Acta* 2004; **357**, 95-102.
- [22] E Szlyk, A Surdykowski, M Barwiolek and E Larsen. Spectroscopy and stereochemistry of the optically active copper(II), cobalt(II) and nickel(II) complexes with Schiff bases N,N'-(1R,2R)-(-)-1,2-cyclohexylenebis(3-methylbenzylideneiminato) and N,N'-(1R,2R)-(-)-1,2-cyclohexylenebis(5-methylbenzylideneiminato). *Polyhedron* 2002; **21**, 2711-7.
- [23] L Mitu, R Natarajan, A Kriza, N Stanica and M Dianu. Synthesis, characterization and antimicrobial activity of Cu(II), Ni(II), Co(II), Zn(II) complexes with isonicotinoylhydrazone-4-benzyloxybenzaldehyde. *Asian J. Chem.* 2009; **21**, 5749-56.
- [24] P Chattopadhyay and C Sinha. Synthesis and characterization of uranyl complexes and their peroxo derivatives with some thio Schiff bases. *Indian J. Chem.* 1996; **35**, 523-6.
- [25] B Dede, I Ozmen and F Karipcin. Synthesis, characterization, catalase functions and DNA cleavage studies of new homo and heteronuclear Schiff base copper(II) complexes. *Polyhedron* 2009; **28**, 3967-74.
- [26] XD Peizhi and Boz. Transition metal complexes of isonicotinoyl-hydrazone-4-diphenylamino benzaldehyde: Synthesis, characterization and antimicrobial studies. *Asian J. Chem.* 2005; **17**, 969.
- [27] D Kivelson and R Neiman. Line shapes in glasses of copper complexes. *J. Chem. Phys.* 1961; **35**, 156-61.
- [28] IM Procter, BJ Hathaway and P Nicholis. The electronic properties and stereochemistry of the copper(II) ion. Part V. The tetra-ammine complexes. *J. Chem. Soc. A* 1969. DOI: doi.org/10.1039/J19690000065.
- [29] S Usha and M Palaniandavar. Influence of chelate-ring size and number of sulfur-donor atoms on spectra and redox behaviour of copper(II) bis(benzimidazolyl) tetra- and penta- thioether complexes. *J. Chem. Soc. Dalton Trans.* 1994; **15**, 2277-83.
- [30] M Sirajuddin, S Ali and A Badshah. Drug-DNA interactions and their study by UV-Visible, fluorescence spectroscopies and cyclic voltammetry. *J. Photochem. Photobiol. B* 2013; **124**, 1-19.